Functional interaction between dynein light chain and intermediate chain is required for mitotic spindle positioning

Melissa D. Stuchell-Brereton[a,*], Amanda Siglin[b,*], Jun Li[a], Jeffrey K. Moore[a], Shubbir Ahmed[c], John C. Williams[b,c], and John A. Cooper[a,†]

[a]Department of Cell Biology and Physiology, Washington University School of Medicine, St. Louis, MO 63110;
[b]Department of Biochemistry and Molecular Biology, Thomas Jefferson University, Philadelphia, PA 19107;
[c]Department of Molecular Medicine, Beckman Research Institute, City of Hope, Duarte, CA 91010

ABSTRACT **Cytoplasmic dynein is a large multisubunit complex involved in retrograde transport and the positioning of various organelles. Dynein light chain (LC) subunits are conserved across species; however, the molecular contribution of LCs to dynein function remains controversial. One model suggests that LCs act as cargo-binding scaffolds. Alternatively, LCs are proposed to stabilize the intermediate chains (ICs) of the dynein complex. To examine the role of LCs in dynein function, we used *Saccharomyces cerevisiae*, in which the sole function of dynein is to position the spindle during mitosis. We report that the LC8 homologue, Dyn2, localizes with the dynein complex at microtubule ends and interacts directly with the yeast IC, Pac11. We identify two Dyn2-binding sites in Pac11 that exert differential effects on Dyn2-binding and dynein function. Mutations disrupting Dyn2 elicit a partial loss-of-dynein phenotype and impair the recruitment of the dynein activator complex, dynactin. Together these results indicate that the dynein-based function of Dyn2 is via its interaction with the dynein IC and that this interaction is important for the interaction of dynein and dynactin. In addition, these data provide the first direct evidence that LC occupancy in the dynein motor complex is important for function.**

Monitoring Editor
Xueliang Zhu
Chinese Academy of Sciences

Received: Jan 27, 2011
Revised: May 17, 2011
Accepted: May 23, 2011

INTRODUCTION

Cytoplasmic dynein is a multisubunit molecular motor that uses ATP hydrolysis to participate in microtubule-based retrograde transport. In higher eukaryotes, dynein is involved in the transport of vesicles and organelles, as well as positioning the mitotic spindle and microtubule organizing centers with respect to the cell cortex. The molecular interactions that underlie dynein's range of functional roles are a topic of current investigation.

Cytoplasmic dynein consists of heavy chain (HC), intermediate chain (IC), light IC (LIC), and light chain (LC) subunits, all of which exist as homodimers in the fully formed complex (Vallee *et al.*, 2004). The HC subunits each contain a microtubule binding domain and six AAA (ATPases associated with diverse cellular activities) ATPase domains that convert the energy from ATP hydrolysis into dynein movement along microtubules (Gee *et al.*, 1997; Koonce, 1997; Samso *et al.*, 1998; Neuwald *et al.*, 1999). The N-terminal "tail" domains of the HC subunits create a scaffold for the LIC and IC components (Habura *et al.*, 1999; Tynan *et al.*, 2000). Finally, the LC subunits bind to the N-terminal region of the ICs (Lo *et al.*, 2001; Mok *et al.*, 2001; Susalka *et al.*, 2002).

The dynein complex works in conjunction with dynactin, a multisubunit complex that is required for dynein function (Muhua *et al.*, 1994; Karki and Holzbaur, 1995; McGrail *et al.*, 1995; Vaughan *et al.*, 1995; Kahana *et al.*, 1998; Sheeman *et al.*, 2003; Schroer, 2004). The central component of the dynactin complex, p150^{Glued}, interacts directly with the N terminus of dynein IC (Karki and Holzbaur, 1995; King *et al.*, 2003). Thus, the N-terminal region of the IC subunit provides a scaffold that facilitates interaction between the dynein and dynactin complexes.

This article was published online ahead of print in MBoC in Press (http://www.molbiolcell.org/cgi/doi/10.1091/mbc.E11-01-0075) on June 1, 2011.

*These authors contributed equally to this work.

†Editorial and Production office communications.

Address correspondence to: John A. Cooper (jcooper@wustl.edu) or John C. Williams (JWilliams@coh.org).

Abbreviations used: HC, heavy chain; HU, hydroxyurea; IC, intermediate chain; LC, light chain; LIC, light IC; SPB, spindle pole body.

The IC subunits also provide a binding surface for the LC subunits. The LC8 and Tctex1 LC families interact with an unstructured region of IC, immediately adjacent to the dynactin binding site (Nyarko *et al.*, 2004; Williams *et al.*, 2007). Despite having no sequence homology, LC8 and Tctex1 are structurally similar (Benashski *et al.*, 1997; Fan *et al.*, 1998, 2001; Liang *et al.*, 1999; Barbar *et al.*, 2001; Williams *et al.*, 2005), and they interact with IC via two exclusive binding sites (Lo *et al.*, 2001; Mok *et al.*, 2001; Rodriguez-Crespo *et al.*, 2001; Varma *et al.*, 2010). Roadblock, a third structurally different LC family member, binds to a helical stretch of the IC in a region downstream of the other two LC binding sites (Susalka *et al.*, 2002; Hall *et al.*, 2010).

The contribution of LCs to dynein function remains an open question. LC8 and Tctex1 interact with multiple dimeric non-dynein-binding partners, including myosin V (Espindola *et al.*, 2000), nNOS (Jaffrey and Snyder, 1996), Pak1 (Vadlamudi *et al.*, 2004; Lightcap *et al.*, 2008), 53BP1 (Lo *et al.*, 2005), Rabies virus P protein (Raux *et al.*, 2000), Fyn (Campbell *et al.*, 1998), Trk receptors (Yano *et al.*, 2001), rhodopsin (Tai *et al.*, 1999), and others. The apparent promiscuity of the LCs led to a model in which LC dimers connect these molecules to dynein for retrograde transport. However, this model is not supported by recent structural and thermodynamic studies, which demonstrate that the IC interacts with LC8 and Tctex1 in precisely the same binding site as their non-dynein-binding partners (Liang *et al.*, 1999; Fan *et al.*, 2001; Navarro-Lerida *et al.*, 2004; Williams *et al.*, 2007). In addition, the fact that the LC subunits are homodimers (Liang *et al.*, 1999; Wu *et al.*, 2005) and contain identical binding grooves allows each LC subunit to bind dimeric IC simultaneously, leading to an energetically favorable bivalent–bivalent interaction (Williams *et al.*, 2007). Deuterium exchange experiments (Williams *et al.*, 2007) and subsequent isothermal titration experiments confirmed the importance of multivalency in LC association with IC (Hall *et al.*, 2009). Moreover, non-dynein LC binding partners are also dimeric, suggesting that they interact with LC dimers in a similar manner.

In an alternate model, LCs interact with dynein and non-dynein-binding partners separately, providing a regulatory function toward dynein, independent of other LC-binding partners. The proximity of the LC and dynactin binding sites on the IC, as well as the local disorder of the IC N terminus, suggest that the LCs may act to stabilize this region of IC to provide regulation of dynein activity. Early studies showed that the biochemical removal of IC/LC subcomplexes from the dynein complex increased ATPase activity of HC/LIC subcomplexes (Kini and Collins, 2001; King *et al.*, 2002). It must be noted, however, that these subcomplexes were unstable, formed aggregates, and exhibited reduced microtubule gliding activity (Gill *et al.*, 1994). On addition of IC/LC subcomplexes, aggregate formation was diminished, suggesting that the IC/LC subcomplexes helped maintain a more native conformation of HC/LIC (King *et al.*, 2002). Together, these data are consistent with a model in which LCs stabilize the dynein structure; however, the mechanism of LC contribution to dynein function remains ambiguous.

Studying the role LCs play in dynein function has been difficult due to multiple non-dynein LC binding partners. Loss of LC often produces pleiotropic effects that confound functional analyses due to the possibility of cellular effects in dynein-independent pathways (Dick *et al.*, 1996a; Varma *et al.*, 2010). In higher eukaryotes, dynein plays a role in multiple processes, making it difficult to separate a specific defect in one process from others. Therefore, to characterize LC contribution to dynein function, we use the budding yeast, *S. cerevisiae*, in which the only known role of cytoplasmic dynein is to position the mitotic spindle during cell division. The current model for dynein function in yeast suggests that the dynein/dynactin complex is first targeted to the plus-ends of microtubules where, by virtue of microtubule dynamics, it probes the bud cortex for docking sites marked by the Num1 protein (Lee *et al.*, 2003, 2005; Moore *et al.*, 2008). Dynein/dynactin is then transferred to the bud cortex, where it applies a force on cytoplasmic microtubules, pulling the spindle and nucleus into the junction between the mother and bud, known as the bud neck.

In this study, we characterize Dyn2 as a member of the budding yeast dynein complex and the homolog of mammalian LC8. The *dyn2* loss-of-function phenotype is less severe than that of heavy chain (*dyn1)* mutants, suggesting that the loss of Dyn2 impairs dynein function without abolishing it. Dyn2 forms a complex with the yeast IC, Pac11, in vivo, and localizes with other dynein components at cytoplasmic microtubule plus-ends. We also identify specific Dyn2 binding sites in Pac11 that, when disrupted, impair dynein function in vivo. We conclude that Dyn2 is required for efficient function of dynein in *S. cerevisiae*. Furthermore, our results suggest that Dyn2 enhances the interaction between dynein and dynactin.

RESULTS

Dyn2 has sequence similarity to the LC8 family of dynein light chains

The putative yeast dynein LC gene, *DYN2/YDR424C/SLC1*, was originally identified by searching the yeast genome for sequences similar to those of the human light chain (Dick *et al.*, 1996b). The Dyn2 amino acid sequence is most similar to the highly conserved LC8 family of metazoan dynein light chains, including LC8 from *Homo sapiens* and *Drosophila melanogaster* (Figure 1A; Dick *et al.*, 1996b; Harrison and King, 2000; Larkin *et al.*, 2007). The C-terminal portion of Dyn2 contains the region of highest similarity to LC8. Moreover, amino acids involved in LC8 dimerization and interaction with IC are highly conserved (Figure 1A, highlighted in red and purple, respectively).

Dyn2 is a member of the yeast dynein pathway

We identified *DYN2/YDR424C* as a potential dynein pathway member in a screen for viable haploid null mutants that display an aberrant nuclear segregation phenotype, which is characteristic of loss of dynein (Lee *et al.*, 2005). Mutations in dynein and its regulators are not lethal; mutant cells can compensate for the absence of bud-directed pulling forces by pushing one spindle pole body (SPB), or yeast microtubule organizing center, into the bud during spindle elongation. In this scenario, the proper alignment of the spindle along the mother-bud axis by the Kar9 pathway is essential for the success of mitosis (Miller and Rose, 1998).

In a nuclear segregation assay, *dyn2*Δ null mutant cells exhibited an increased frequency of mispositioned spindles and/or multiple nuclei when compared with wild-type cells; however, the phenotype was not as strong as that seen for null mutants of the dynein heavy chain, *dyn1*Δ (Figure 1B). To verify that the *dyn2*Δ phenotype is due to a disruption of the dynein pathway and not the Kar9 pathway, we performed epistasis experiments with double mutant strains containing *dyn2*Δ in combination with either *dyn1*Δ or *kar9*Δ. In comparison to wild-type cells, *dyn2*Δ*kar9*Δ double mutant cells exhibited a growth defect, whereas the *dyn2*Δ*dyn1*Δ double mutant cells exhibited normal growth, placing *dyn2* in the dynein pathway (Figure 1C). In addition, the growth defect of *dyn2*Δ*kar9*Δ double mutants was less severe than that of *dyn1*Δ*kar9*Δ mutants (Figure 1C). These data indicate that Dyn2 functions in the dynein pathway, not the Kar9 pathway, and that Dyn2 is important but not essential for dynein activity.

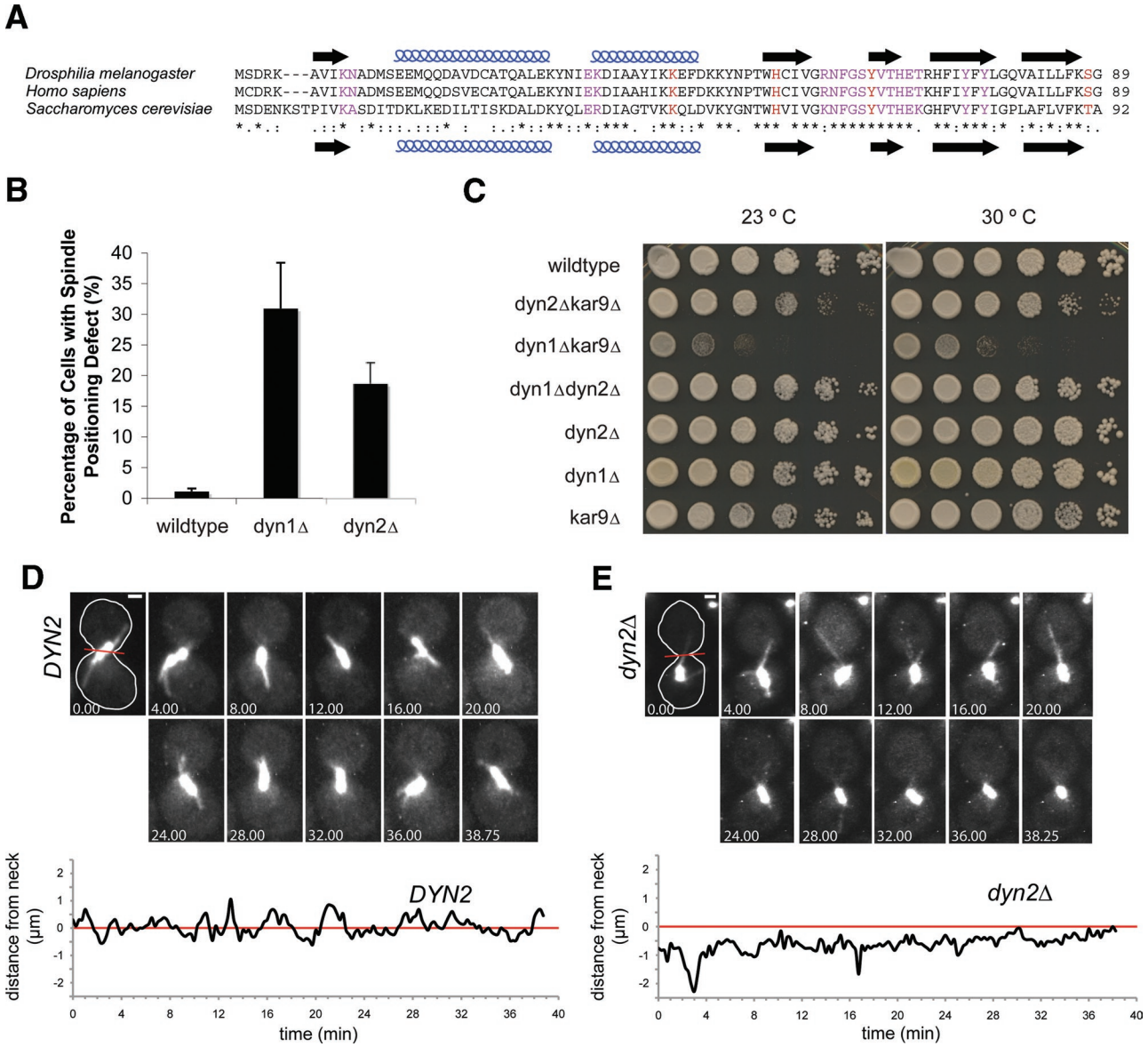

FIGURE 1: Dyn2 is the yeast LC8 homologue. (A) Dyn2 is highly similar to the LC8 family of mammalian dynein light chains, based on sequence alignment and secondary structure prediction. Dyn2 is 46.7% identical and 71.7% similar to *H. sapiens* LC8 (Accession number Q96FJ2), 47% identical and 72% similar to *D. melanogaster* LC8 (Accession number NP_726942.1), and 46% identical and 71% similar to *Mus musculus* LC8 (Accession number NP_080832). Amino acids highlighted in red are involved in light chain dimerization, and amino acids highlighted in purple are involved in LC8 interaction with the dynein IC. (B) The requirement of Dyn2 for dynein function was tested in vivo using a single–time point nuclear segregation assay. yJC5919, yJC5603, and yJC7259 strains were used. Error shown is SD. (C) Epistasis experiments place Dyn2 in the dynein pathway, not the Kar9 pathway. yJC2588, yJC3601, yJC3607, yJC3754, yJC3756, and yJC3832 strains were used. (D, E) Analysis of preanaphase spindle movement in representative HU-arrested wild-type cells (panel D, yJC5919) and *dyn2*Δ cells (panel E, yJC7259). Images represent single time points at 4-min intervals. Bar is 1 μm. Graphs represent the distance that the daughter-bound SPB is from the bud neck (0) at each time point.

To further examine Dyn2 involvement in the dynein-dependent spindle positioning pathway, we studied the ability of dynein to move the spindle through the bud neck in the presence and absence of Dyn2. To specifically assess spindle movement based on force exerted on cytoplasmic microtubules, and not force generated by spindle elongation, we prevented anaphase spindle elongation by arresting cells with hydroxyurea (HU). Time-lapse imaging of wild-type cells revealed robust movement of GFP-Tubulin (Tub1)–labeled spindles across the bud neck (Figure 1D; Supplemental Video S1). However, cells lacking Dyn2 failed to pull the spindle or SPB across the neck (Figure 1E; Supplemental Video S2). In a quantitative analysis of these movies, described in *Materials and Methods*, spindle movements across the neck were scored. In a fixed period of time, 37% (n = 93) of wild-type cells and 5% (n = 121) of mutant cells displayed such movement. These data suggest that Dyn2 is important for dynein-mediated spindle movement across the bud neck.

Dyn2 colocalizes with dynein

We analyzed Dyn2 localization by assessing the colocalization of Dyn2 with previously characterized components of the yeast cytoplasmic dynein complex. Yeast HC, Dyn1, and IC, Pac11, localize to the plus-ends of cytoplasmic microtubules, to sites near SPBs, and

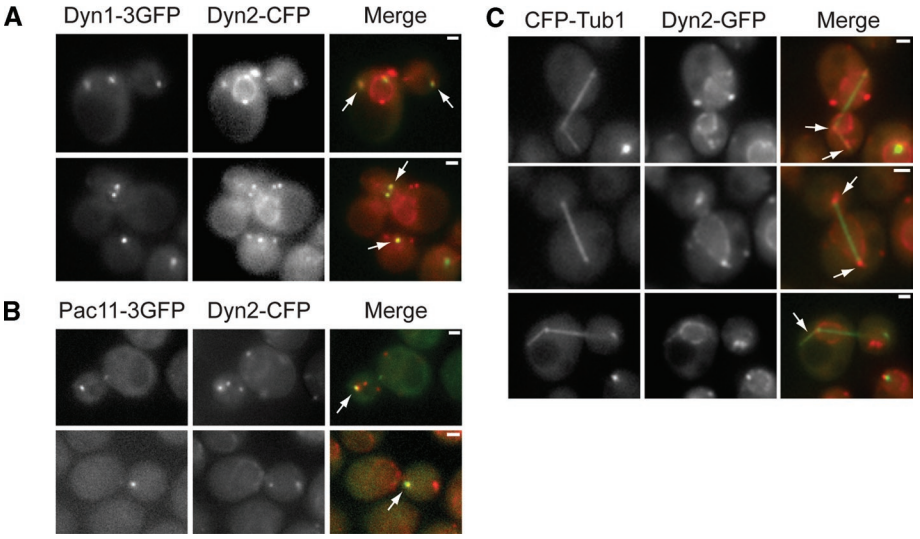

FIGURE 2: Dyn2 localization in cells. (A) Dyn2 colocalizes with dynein heavy chain, Dyn1, at SPBs and cytoplasmic foci and (B) dynein IC, Pac11, at cytoplasmic foci. (C) Dyn2 colocalizes with tubulin at SPBs, along cytoplasmic microtubules, at the plus-ends of cytoplasmic microtubules, and at the nuclear envelope. Strains were yJC4883 (A), yJC4966 (B), and yJC4371 (C). White arrows denote sites of colocalization. Bar is 1 μm.

to stationary cortical foci (Lee *et al.*, 2003, 2005; Sheeman *et al.*, 2003). Using Dyn2-CFP (a functional fusion, described in *Materials and Methods*) in combination with either Dyn1–3XGFP or Pac11–3XGFP (Lee *et al.*, 2003, 2005), we observed Dyn2 colocalization with both Dyn1 and Pac11 in foci reminiscent of plus-ends and SPBs (Figure 2, A and B). Indeed, observation of Dyn2-GFP (a functional fusion, described in *Materials and Methods*) in cells expressing CFP-labeled microtubules confirmed that Dyn2 localizes near the SPBs, at cytoplasmic microtubule plus-ends and along the lengths of cytoplasmic microtubules (Figure 2C).

In a previous study, yeast Dyn2 was found to associate with nuclear pore complexes (NPCs) and peroxisomes (Stelter *et al.*, 2007). We confirmed colocalization of Dyn2 with NPCs in wild-type and *nup133*Δ cells and observed a decrease in the number of cytoplasmic Dyn2 punctae in the absence of Pex14 (Supplemental Figure 1). The fact that Dyn2 interacts with multiple non-dynein-binding partners raised the question of how Dyn2 contributes to dynein function. To address this question, we studied the interaction of Dyn2 with the yeast IC, Pac11.

Yeast IC/Pac11 contains two predicted LC8 binding sites

A direct interaction between LC8 and IC has previously been characterized in vitro using LC and IC homologues from higher eukaryotes (Makokha *et al.*, 2002; Nyarko *et al.*, 2003, 2004; Benison *et al.*, 2007; Williams *et al.*, 2007; Hall *et al.*, 2008, 2009). To investigate the possibility of such an interaction in yeast, we first analyzed the sequence of Pac11 to identify potential LC8 binding sites. Nearly all LC8 binding sites include a conserved glutamine flanked by threonine or hydrophobic residues (Val, Ile) and are generally predicted to contain a β-strand secondary structure (Gross, 2004; Lajoix *et al.*, 2004; Figure 3A). In addition, metazoan dynein ICs contain a tyrosine at position i-5 from the conserved glutamine residue in the LC-binding site. Based on this metric, the sequence $_{76}$TYDKGIQTD$_{84}$ in Pac11 is nearly identical to the human IC binding motifs, $_{148}$SYSKETQTP$_{156}$ (IC1: GenBank Accession number NP_001129028) and $_{155}$TYTKETQTP$_{163}$ (IC2: GenBank Accession number NP_001369) (Figure 3B). We also observed a second potential binding site on the N-terminal side of the first site. Residues $_{47}$VSVSVQTD$_{54}$ also contain an invariant glutamine flanked by threonine and valine (Figure 3B), and a secondary structure prediction algorithm also suggests the structure is a β-strand (data not shown; Rost and Sander, 1994). In addition, alignment of these sites with the previously identified dynein light chain–interacting domain (DID; Stelter *et al.*, 2007) (Figure 3C) shows conservation between known Dyn2 binding motifs and the two probable sites identified in Pac11. We will hereafter refer to the potential binding sites found at $_{47}$VSVSVQTD$_{54}$ and $_{76}$TYDKGIQTD$_{84}$ as site 1 and site 2, respectively.

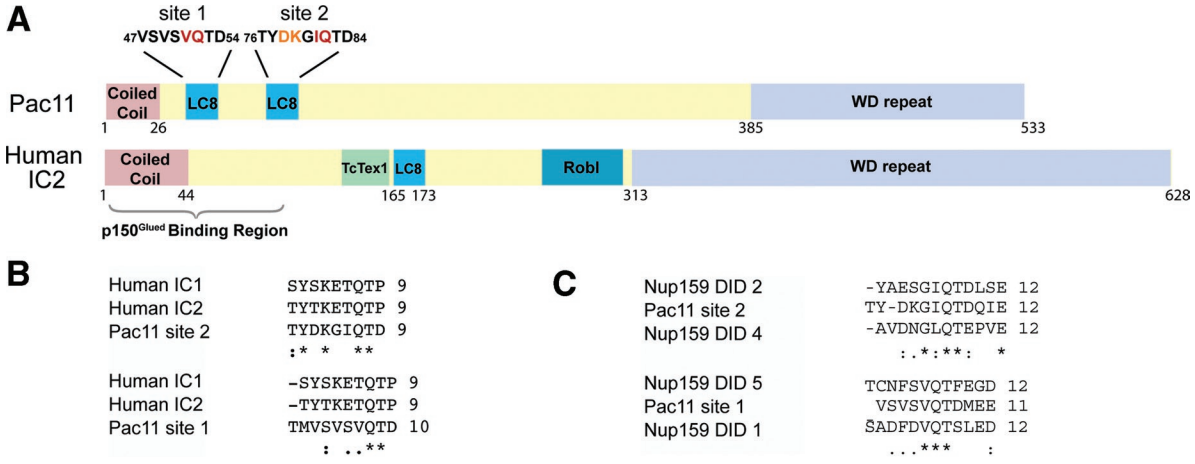

FIGURE 3: Dynein IC domain structure and light-chain binding sites. (A) Domain structure of Pac11 and human IC (IC2C isoform, GenBank Accession number NP_001369). Pac11 contains a short predicted coiled-coil domain followed by two putative LC8 binding sites and a C-terminal WD repeat domain. Domains determined using NCBI BLAST. Sequences of the predicted Dyn2/yLC8 binding sites on Pac11 are shown above schematic. (B) The two putative Dyn2/yLC8 binding sites identified in Pac11, site 1 and site 2, are aligned with human LC8 binding sites in human IC (isoforms IC1 and IC2) (C) and the Dyn2 binding sites identified in Nup159 (Stelter *et al.*, 2007). Alignments created using ClustalW2 at EMBL-EBI (Larkin *et al.*, 2007).

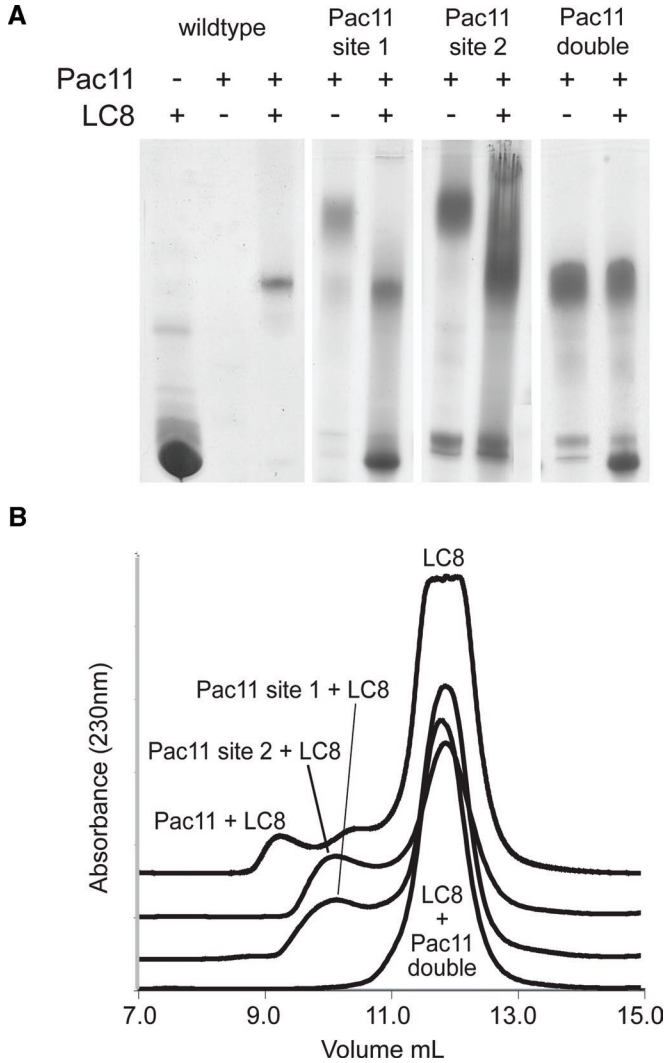

FIGURE 4: Biochemical analysis of putative LC8-binding sites. (A) Native gel analysis of *Drosophila* LC8 and its interaction with wild-type Pac11 1–86aa fragment, Pac11 site 1 mutant 1–86aa, Pac11 site 2 mutant 1–86aa, and Pac11 double mutant 1–86aa. (B) Analysis of *Drosophila* LC8 and interaction with Pac11 fragments by size exclusion chromatography. The combination of the Pac11 1–86aa fragment and LC8 elutes at 9.3 ml. Both the single site mutants (sites 1 and 2) elute at 10.2 and 10.1 ml, respectively. No association is seen between the Pac11 double mutant fragment and LC8.

Light chain binding sites are necessary for LC–IC interaction in vitro

To test the putative LC8 binding sites in Pac11, we expressed and purified a Pac11 fragment that spans residues 1–86. Pac11 associated with both yeast Dyn2 (data not shown and Supplemental Figure 2) and *Drosophila* LC8 (Figure 4, A and B), which has extensive sequence similarity with Dyn2 (Figure 1A), by native PAGE and analytical size exclusion chromatography (SEC), confirming that Pac11 contains conserved LC8-binding sites. To determine the overall stoichiometry, we conducted sedimentation equilibrium measurements and obtained a calculated mass of 54336 ± 600 kDa (χ^2 = 3.4) for the wild-type Pac11–LC8 complex (Figure 5A and Table 1). The theoretical mass of two LC8 dimers (4 monomers) and two Pac11 peptides is 61,566 kDa. The difference in calculated and theoretical molecular weight likely reflects equilibrium between the full complex and one or more individual components (e.g., 4[LC8] + [Pac11] + [Pac11] <-> [2LC8$_2$ Pac11$_2$]). We also observe that the Pac11 1–86 fragment was monomeric with a calculated molecular weight of 11,557 ± 527 kDa (χ^2 = 3.2) (Figure 5E).

In these association experiments, the mixing time was critical to the formation of the complex. Specifically, SEC and native PAGE experiments performed immediately following the mixture of Pac11 peptides and LC8 did not produce a fully formed complex, whereas longer mixing periods (>1 h) did support complex formation. We attribute this to the number of potential protein binding configurations, many of which are not productive.

To further test the proposed LC8 binding sites in Pac11, we introduced point mutations into Pac11 that are predicted to disrupt the IC–LC8 interaction based on previous studies in mammalian systems (Figure 3A, highlighted in red; Lajoix *et al*., 2004; Lightcap *et al*., 2008). We generated a VQ(51,52)DA mutation at site 1 and a IQ(81,82)DA mutation at site 2. A double mutant was also generated (containing mutations at both sites). Both single-site Pac11 point mutants associated with *Drosophila* LC8 in native PAGE and SEC assays, whereas the double-site mutant did not (N.B. mixing time was >1 h; Figure 4, A and B). To test the stoichiometry, sedimentation equilibrium studies were conducted. For the double mutant, we found no evidence of association (Figure 5B and Table 1). Specifically, the monomeric weight of Pac11 was fixed, whereas the molecular weight of *Drosophila* LC8 was fit. These data fit to a molecular weight of 19,857 ± 435 kDa (χ^2 = 1.1) (the dimeric weight of LC8), suggesting only LC–LC interaction. In the presence of either the VQ(51,52)DA or IQ(81,82)DA mutations alone, we observed a calculated mass of 36,115 ± 327 kDa (χ^2 = 2.7) and 34,258 ± 548 kDa (χ^2 = 4.1), respectively, indicating that both sites are important for LC8 binding and complex formation (Figure 5, C and D, and Table 1). Taken together, these data demonstrate biochemically that Pac11 contains two LC8 binding sites.

Light chain binding sites affect LC–IC association in vivo

To determine whether the putative Dyn2/LC8 binding sites in Pac11 are important in the context of full-length proteins in cells, we tested the Dyn2–Pac11 interaction by immunoprecipitation from cell extracts. Point mutations were introduced into the *PAC11* chromosomal locus at the putative Dyn2 binding sites using previously described methods (Moore *et al*., 2009), disrupting one site singly (site 1: VQ(51,52)DA, or site 2: DK(78,79)AA,IQ(81,82)DA) or both sites simultaneously. Immunoprecipitation of TAP-tagged Pac11 from cell lysates followed by immunoblotting for Myc-tagged Dyn2 (a functional fusion, described in *Materials and Methods*) revealed association of wild-type Pac11 with Dyn2 (Figure 6A). The mutations at site 2 abolished the interaction with Dyn2, the mutations at site 1 reduced the interaction with Dyn2, and the double mutant resembled the site 2 single mutant (Figure 6A). These data provide evidence that site 2 is necessary and sufficient for Dyn2 association in the context of full-length proteins in cells. In contrast, site 1 contributes to the Dyn2–Pac11 interaction but is not necessary.

Light chain binding sites promote efficient spindle positioning

We next addressed whether the Dyn2 binding sites in Pac11 are required for dynein function in cells by scoring the position of mitotic spindles in *pac11* point mutant cells (Figure 6B). Cells harboring the mutation at site 2 alone exhibited defects at a level similar to *dyn2*Δ null mutant cells ($p = 0.11$). In contrast, mutation of site 1 had a smaller, yet still significant, defect ($p < 0.01$, compared with

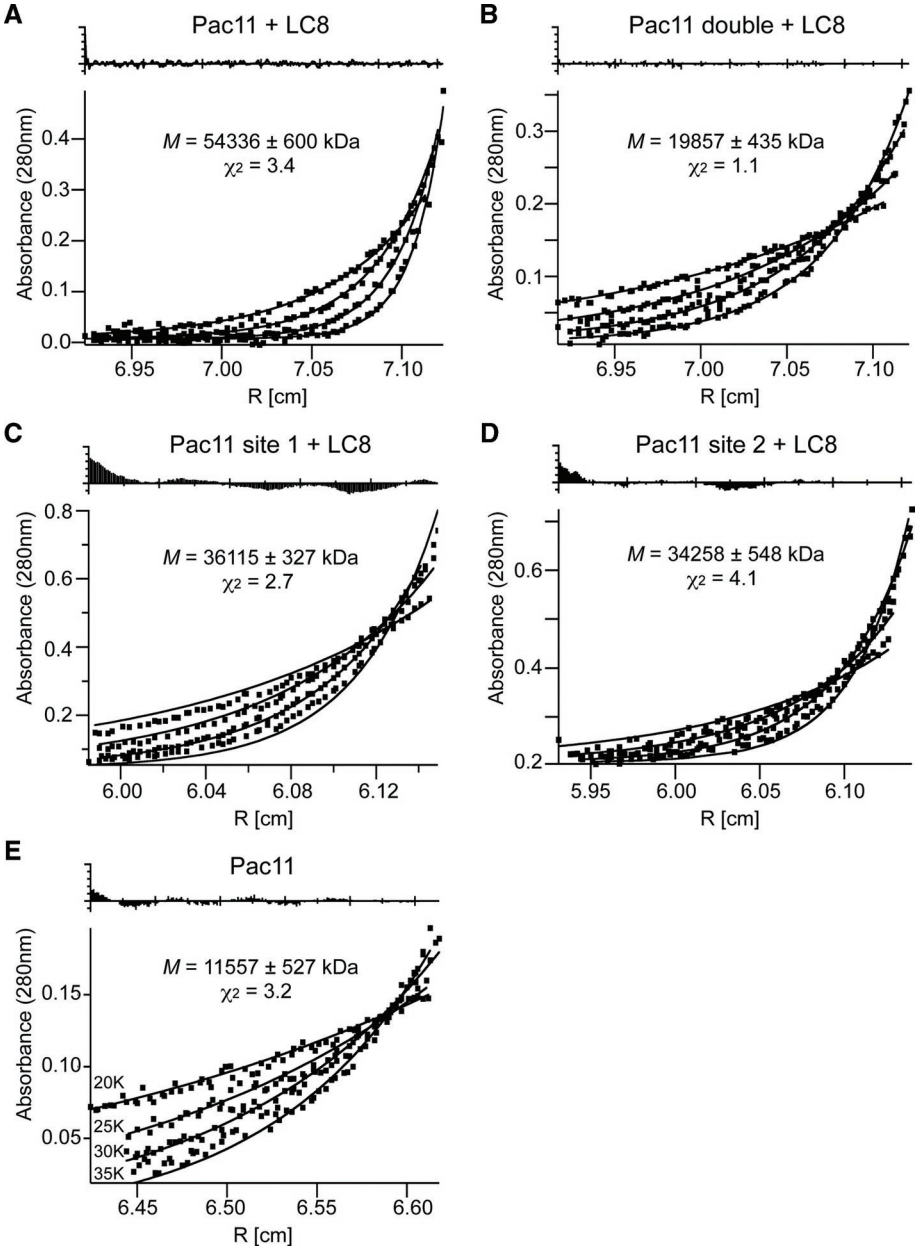

FIGURE 5: Sedimentation equilibrium using analytical ultracentrifugation. (A) Radial absorbance (280 nm) of LC8 and wild-type Pac11 at 20, 25, 30, and 40K rpm. The data were fitted as a single species with the molecular weight as the only variable parameter. The resulting molecular weight is 54 kDa, consistent with 2 LC8 dimers (20.6 kDa) and two wt Pac11 fragments (10 kDa each) with some association/dissociation; (B) LC8 and the Pac11 double mutant fragment were mixed at 2:1 stoichiometry and equilibrated overnight before the analysis. Fitting the data as a single species did not produce an adequate fit. Fitting the data as two noninteracting species at the appropriate concentrations and molar extinction coefficients afforded a fit to the dimeric weight of LC8 and monomeric weight of Pac11, indicating no interaction. (C) Same as (A) but using the Pac11 site 1 mutant fragment. (D) Same as (A) but using the Pac11 site 2 mutant fragment. (E) Radial absorbance (280 nm) of Pac11 indicates that the 1–86 fragment of Pac11 is monomeric with a calculated molecular weight of 11,557 ± 527 kDa ($\chi^2 = 3.2$).

wild-type cells). When both sites were mutated, an enhanced phenotype was seen compared with either of the single site mutations ($p < 0.01$, compared with site 1 and site 2). An enhanced phenotype was also apparent when comparing the spindle positioning defects of the double mutant cells with those seen in *dyn2*Δ null mutant cells ($p < 0.01$), suggesting that mutations in this region of IC may also affect dynein function independent of Dyn2. To test the hypothesis that the role of these sites is to bind Dyn2, we combined the *dyn2*Δ null mutation with the *pac11* point mutations. Each of the single-site combinations exhibited a level of defect similar to the *dyn2*Δ mutant alone ($p = 0.17$, compared with site 1/*dyn2*Δ, $p = 0.16$, compared with site 2/*dyn2*Δ); however, the double site/*dyn2*Δ mutant showed an enhanced defect ($p < 0.01$, *dyn2*Δ null mutant compared with the double mutant/*dyn2*Δ). This enhancement is similar to that seen for the double mutant cells alone (*dyn2*Δ null mutant compared with the double mutant, $p < 0.01$). In sum, both Dyn2 binding sites on Pac11 contribute to dynein function in vivo.

To determine the effect of inhibiting the Dyn2–Pac11 interaction on dynein activity in a more sensitive functional assay, we assayed the movement of spindles across the bud neck in movies of cells arrested with HU (Figure 7 and Supplemental Videos S3–S6). Whereas wild-type cells exhibited robust spindle movement through the bud neck (37%, n = 93; Figure 1D, Supplemental Video S1), disruption of either Dyn2-binding site abrogated spindle movement through the bud neck (3% for site 1, n = 35, 0% for site 2, n = 28, 0% for the double mutant, n = 28), similar to *pac11* (1%, n = 70; Figure 7A, Supplemental Video S3) and *dyn2* (5%, n = 121; Figure 1E, Supplemental Video S2) null mutant strains. Together, these results indicate that Dyn2 associates with two sites on Pac11 and that both interactions are important for dynein-dependent spindle positioning in yeast.

The interaction of LC and IC is required for targeting dynactin to plus-ends

We next addressed whether the spindle positioning defect observed in the *pac11* mutants was due to a decrease in the amount of dynactin and/or dynein at the plus-ends of cytoplasmic microtubules. We analyzed the fluorescence intensity of dynamitin and dynein HC at plus-ends prior to mitosis, using Jnm1-tdimer2 and Dyn1–3XGFP fusion proteins expressed from the endogenous loci. Jnm1-tdimer2 fluorescence intensity was decreased at plus-ends in *dyn2*Δ cells compared with wild-type cells ($p = 0.0001$, Figure 8A) consistent with previous results (Moore *et al.*, 2008). For each of the *pac11* mutant strains, there was also a significant decrease in Jnm1-tdimer2 fluorescence intensity compared with wild-type cells ($p < 0.004$, Figure 8A). The intensity values in the *pac11* mutants were similar to those of the *dyn2* mutant, suggesting that dynactin localization to plus-ends depends on the

Pac11 construct	Calculated mass (Da)	Complex stoichiometry	Theoretical mass (Da)
Wild-type Pac11	54,336 ± 600	2 Pac11 : 4 LC8	61,566
Pac11-site 1	36,115 ± 327	2 Pac11 : 2 LC8	40,854
Pac11-site 2	34,258 ± 548	2 Pac11 : 2 LC8	40,854
Pac11 double mutant	19,857 ± 435	0 Pac11 : 2 LC8	20,748
Wild-type Pac11 alone	11,557 ± 527	1 Pac11 : 0 LC8	10,053

Wild-type and mutant Pac11 constructs were mixed with *Drosphila* LC8 (except where indicated) prior to analytical ultracentrifugation (described in *Results* and shown in Figure 5). Based on the calculated masses of these protein mixtures, we predicted the stoichiometry of the Pac11–LC8 complexes in vitro.

TABLE 1: Stoichiometries of complexes of Pac11 with LC8.

LC–IC interaction. In contrast, no significant changes were seen for Dyn1–3XGFP intensity levels in *dyn2*Δ and site 1 mutant cells ($p = 0.3$ and $p = 0.8$, respectively, when compared with wild-type cells, Figure 8B; Moore *et al.*, 2008). We did observe a significant decrease in Dyn1–3XGFP intensity levels in both the site 2 and double mutant cells ($p = 0.005$ and $p = 0.0001$, respectively, Figure 8B), suggesting that the site 2 point mutations may also impair dynein function independent of its effects on the LC–IC interaction. These data are consistent with the association of LC with IC being important for dynein function and suggest that the role of LC is to promote the recruitment of dynactin to the dynein complex.

DISCUSSION

In this study, we used genetic analysis, localization studies, biochemical characterization, and in vivo assays of dynein activity to examine the function of the LC8 homologue, Dyn2. Our results demonstrate that null mutations in Dyn2 produce a less severe defect than null mutations in dynein heavy chain, suggesting that dynein retains some function in the absence of Dyn2. Dyn2 localizes to microtubules in vivo through its interaction with the yeast IC, Pac11. We find that Dyn2 binds directly to two sites in Pac11, and in vivo assays indicate that both sites are important for dynein function. Finally, we show that the incorporation of Dyn2 into dynein is important for recruiting the dynactin complex. Together, our results support a model in which the role of LC8/Dyn2 is to promote the formation of the dynein–dynactin complex.

Although both Dyn2 binding sites on Pac11 are important for dynein function, disrupting either site produced differential effects, depending on the sensitivity of the assay. In single–time point nuclear segregation assays, mutating site 1 produced a small effect, mutation of site 2 produced a moderate effect, and simultaneous mutation of both sites conferred an additive effect, which was worse than site 2 alone (Figure 6B). In contrast, in the HU-arrest experiments, which are more sensitive assays of dynein function in the absence of other spindle-positioning mechanisms, each Pac11 single-site mutation severely affected dynein function to a level similar to that found in the Pac11 double-site mutant and the null mutants (Figures 1 and 7). We conclude that, although the disruption of site 2 causes greater impairment of dynein, both sites are necessary for full dynein function. Consistent with this, each of the Pac11 binding sites is important for recruiting dynactin; single-site mutants exhibited defects indistinguishable from the double mutant and the *dyn2*Δ null mutant. Thus, we speculate that Dyn2 is likely to occupy both sites on the Pac11 molecule.

Similar to mammalian LC8, Dyn2 interacts with multiple nondynein proteins, raising the possibility that Dyn2 might act as a bridge between dynein and cargo. However, previously reported data, together with our results, do not support such a role for Dyn2. First, the presence of a bivalent binding site in LC8 interacting proteins is important for LC8 association (Williams *et al.*, 2007; Hall *et al.*, 2009), suggesting that an LC8 dimer binds to two IC sites, rather than linking cargo to IC in trans. This is also true for Dyn2 at the nuclear pore complex, based on the observation that a monomeric Dyn2 (H58K mutant) does not associate with the Nup159 DID polypeptide (Stelter *et al.*, 2007). Second, other components of the dynein complex do not colocalize with Dyn2 binding partners found at nuclear pore complexes or peroxisomes (Figures 2, B and C). Furthermore, viable null mutations in the non-dynein-binding partners Clb2 (Breitkreutz *et al.*, 2010), Pex14 (Stelter *et al.*, 2007), and Prk1 (Breitkreutz *et al.*, 2010) do not exhibit spindle-positioning defects, suggesting that dynein function does not depend on these interactions (J.L.i data not shown). This argues against a model where Dyn2 dimers connect non-dynein-binding partners to the dynein complex.

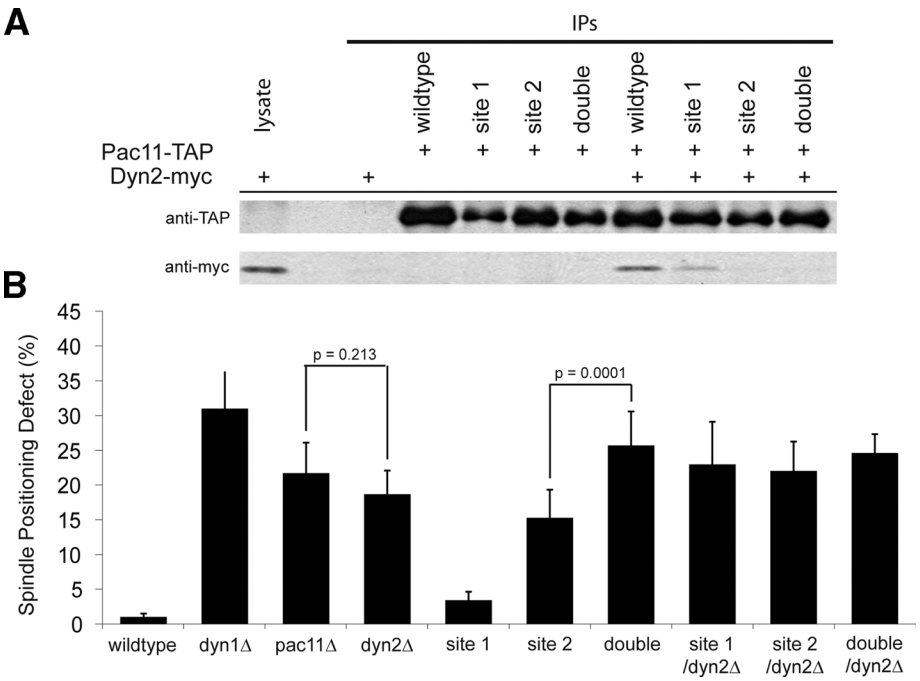

FIGURE 6: Functional analysis of putative Dyn2 binding sites in vivo. (A) TAP-tagged Pac11 constructs were used in a pull-down assay to test the association of Dyn2–13Xmyc with wild-type and mutants forms of Pac11. Strains were yJC7271 through yJC7278. (B) Single–time point nuclear segregation assay for dynein function in cells. Data is averaged from six or nine independent experiments: ~300 cells were counted per experiment per strain. Error shown is SD. Strains were yJC5919, yJC5603, yJC6354, yJC7259, yJC6376, yJC6375, yJC6377, yJC7261, yJC7262, and yJC7263.

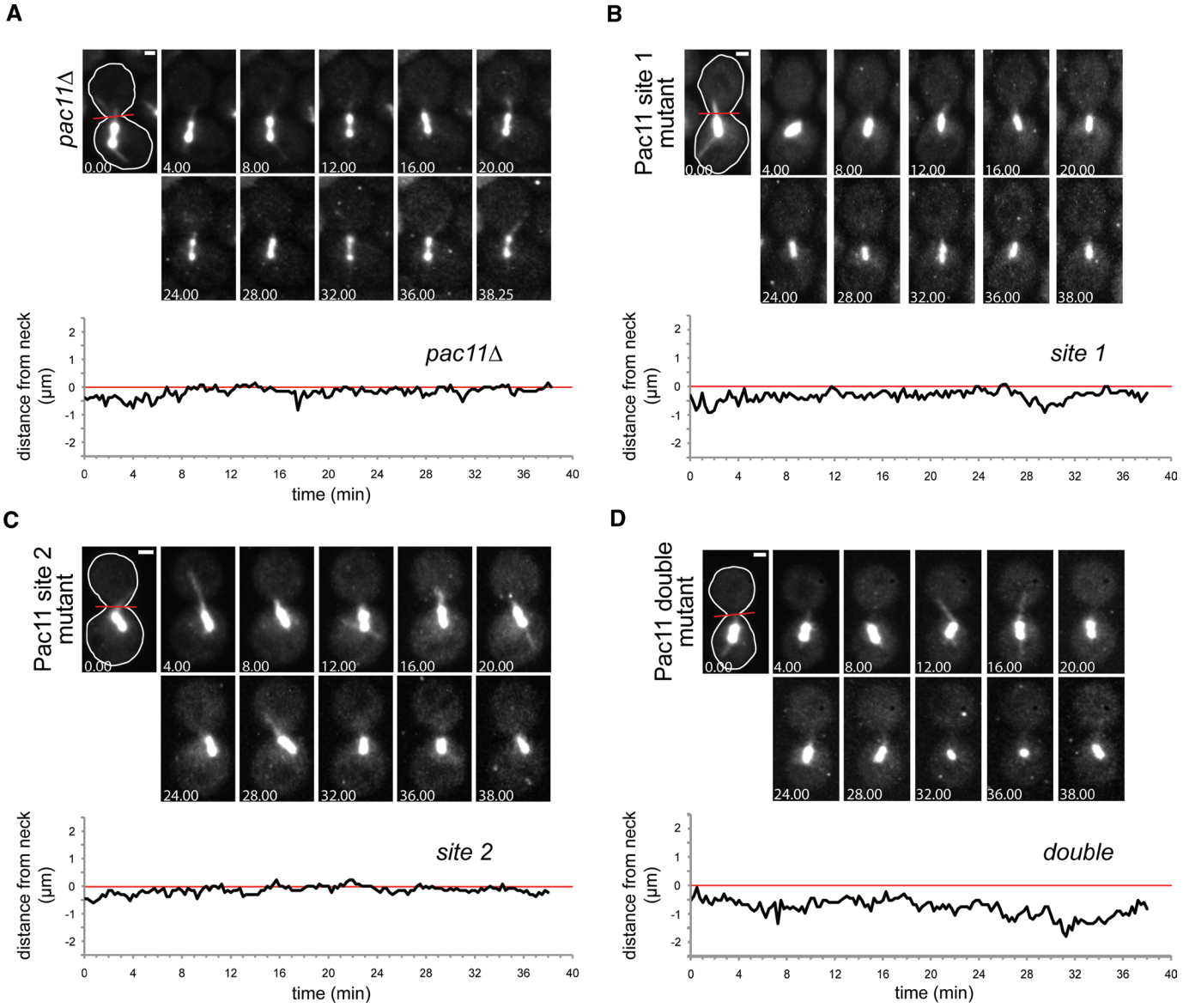

FIGURE 7: Preanaphase spindle dynamics in HU arrested *pac11* mutant cells. Cells expressing GFP-tubulin (Tub1) were arrested in S phase using HU, and preanaphase spindle dynamics were analyzed over time. Images (above) represent single time points at 4-min intervals. Bar is 1 μm. Graphs (below) represent the distance (μm) that the daughter-bound SPB is from the bud neck (0) at each time point. (A) *pac11*Δ (yJC6354), (B) Pac11 site 1 mutant (yJC6376), (C) Pac11 site 2 mutant (yJC6375), (D) Pac11 double mutant (yJC6377).

How might LC8 contribute to dynein–dynactin complex formation? On the basis of the results presented here and previous studies, we favor a model where LC8 plays a role as a structural regulator for the N terminus of IC, which, in turn, enhances the interaction between IC and $p150^{Glued}$. This model is consistent with our finding that Dyn2 is important but not absolutely necessary for dynactin recruitment and overall dynein function. The N terminus of IC is intrinsically disordered yet contains binding sites for the $p150^{Glued}$ subunit of dynactin, Nip100 in yeast (Vaughan and Vallee, 1995; King *et al.*, 2003; Nyarko *et al.*, 2004). Therefore, the binding of LC8 to IC may stabilize and orient the N terminus of IC, such that it promotes interaction with $p150^{Glued}$. This might also explain why Pac11 possesses multiple LC8/Dyn2 binding sites. In the nuclear pore complex, the protein Nup159 contains five tandem Dyn2 binding sites that lie in an unstructured region situated between the N-terminal Phe-Gly repeats and the C-terminal coiled-coil domain. The Nup159 DID/Dyn2 complex forms a rigid rod-shaped structure that is presumed to project the N-terminal Phe-Gly repeats of Nup159 into the cytoplasm, making them accessible to nuclear transport proteins (Stelter *et al.*, 2007). We speculate that these features are conserved in Pac11, and that interaction with Dyn2 may enhance the binding of Nip100 at an adjacent site in Pac11, thereby promoting dynein–dynactin complex formation.

MATERIALS AND METHODS

Molecular biology/plasmid construction

PAC11/YDR488C (Nucleotide Accession number: NM_001180796) base pairs 1–258 were amplified from yeast genomic DNA and inserted into the *Bam*HI and *Xho*I restriction sites of pGEX-6p vector. Standard site-directed mutagenesis protocols were used to mutate residues 51/52 VQ to DA and 81/82 IQ to DA. A quadruple mutant was also generated using the Pac11 81/82 mutant cDNA as a template and incorporating the 51/52 mutations by site-directed

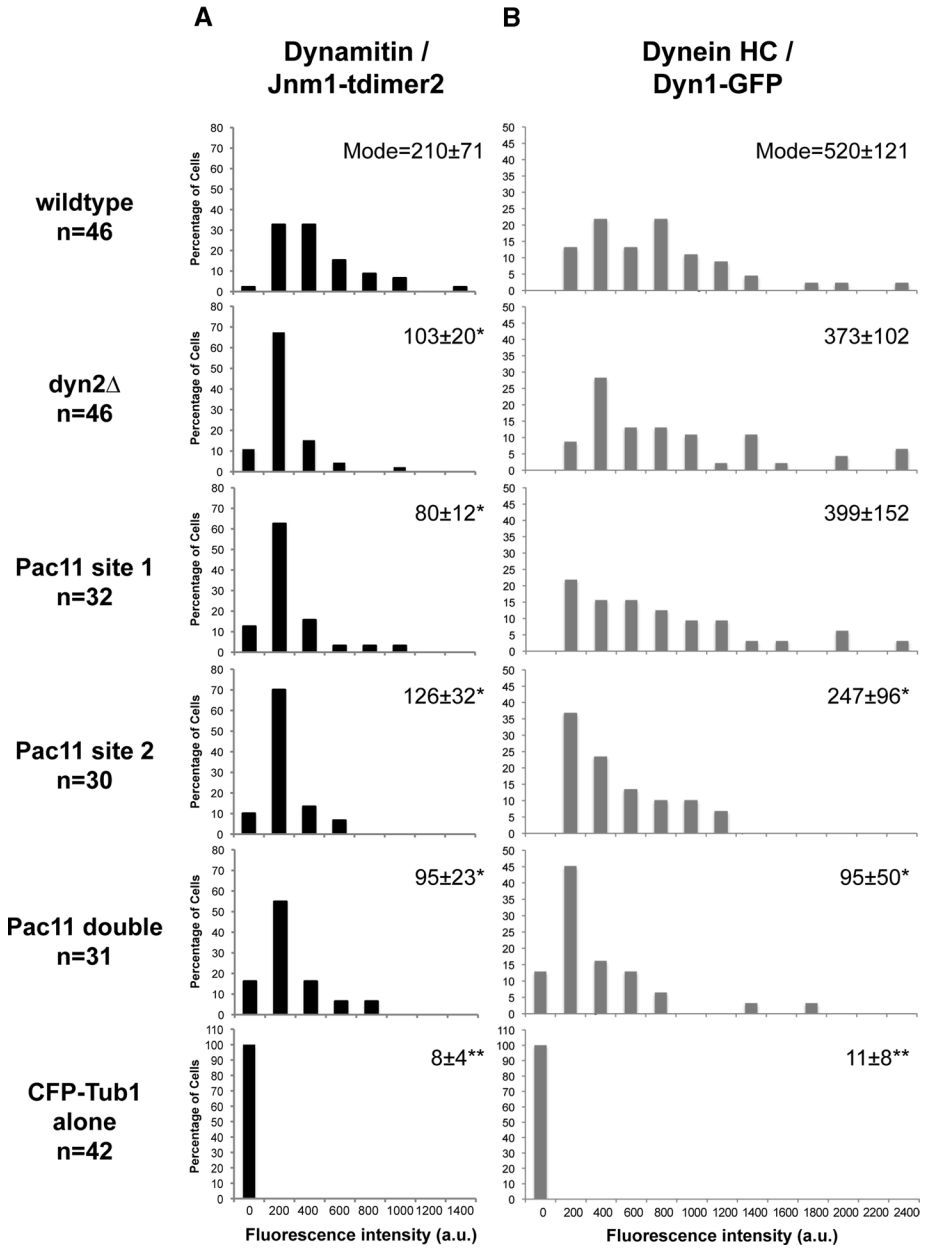

FIGURE 8: Fluorescence intensity measurements of (A) Dynamitin/Jnm1 and (B) Dynein HC/Dyn1 at the plus-ends of microtubules in *pac11* mutant cells. Histograms represent the percentage of cells containing Jnm1 or Dyn1 foci displaying fluorescence intensity at bud-proximal microtubule plus-ends in G_2/M cells, identified by spindle length and grown in log-phase cultures. Microtubule ends were identified in the CFP-Tub1 image, and intensity measurements were taken from the corresponding plane of the GFP or tdimer2 stack. Wild-type and mutant cells are expressing CFP-tubulin (Tub1), Jnm1-tdimer2, and Dyn1–3XGFP. Control cells are expressing CFP-tubulin alone. Modes calculated for each data set are listed in each upper right corner (* represents data sets that are significantly different from respective wild-type data sets ($p \leq 0.005$), and ** represents data sets that are significantly different from all other data sets collected ($p \leq 0.0004$).) Strains were yJC5668, yJC7354, yJC7355, yJC7356, and yJC7358.

mutagenesis. *DYN2/YDR424C/SLC1* (Nucleotide Accession number: NM_001180732) base pairs 1–276 were amplified from yeast genomic DNA and cloned into pET28b-His6-SMT3. The cloning was confirmed by DNA sequencing.

Recombinant protein expression and purification

All constructs were expressed in BL21 Star(DE3) cells (Invitrogen, Carlsbad, CA) and induced at $OD_{600} = 0.5–0.7$ with 250 μM IPTG for 3–4 h. The cells were lysed by French press and clarified at 18,000 rpm at 4°C for 40 min.

Pac11 1-86-GST construct. The clarified lysate was loaded onto a glutathione sepharose column (GE Healthcare, Waukesha, WI) and eluted with 3 mg/ml glutathione, 50 mM Tris, pH 8.0, 1M NaCl, 1 mM EDTA, and 1 mM dithiothreitol (DTT). The eluted GST tag fusion protein was then cleaved from the Pac11 1–86 by cutting with PreScission protease (GE Healthcare). The GST Pac11 mixture was then loaded onto a Superdex 75 prep grade column (GE Healthcare Life Sciences). Pac11 1–86 VQ51,52DA, IQ81,82DA, and VQ51,52DA/IQ81,82DA were prepared and purified in a similar manner.

Dyn2–6XHis-SMT construct. The clarified lysate was passed through a Ni-NTA agarose (QIAGEN, Valencia, CA) column. Bound protein was eluted using a gradient of 1× phosphate-buffered saline (PBS) (137 mM NaCl, 2.7 mM KCl, 4.3 mM, Na2HPO4, 1.47 mM KH2PO4, pH 7.4) containing imidazole. The eluted 6xHis-SMT tag fusion protein was cleaved with ubiquitin-like protease (Ulp-1) for 2 h at 4°C and then passed through a second Ni-NTA agarose column to remove the tag. The flow-through fraction was dialyzed against 50 mM Tris, 100 mM NaCl, 1 mM DTT, 1 mM EDTA, pH 9.0, and further purified using a Superdex 75 prep grade column (GE Healthcare) in the same buffer. Final polishing was done using a Mono-Q column (5/50 GL; GE Healthcare). *Drosophila* LC8 was purified as described previously (Williams *et al*., 2007).

In vitro protein interaction assays/ complex formation

Purified Pac11 fragment was incubated with *Drosophila* LC8 at 25°C for 1 hour and subsequently loaded onto a Superdex 200 10/300 GL (GE Healthcare). The formation of the complex was verified by SDS–PAGE. For the native PAGE interaction studies between WT Pac11 1–86 and LC8, Pac11 was in 2 M excess of LC8. For the native PAGE interaction studies between mutant Pac11 1–86 constructs and LC8, LC8 was in 4 M excess of Pac11. For the SEC interaction studies, 100 μM Pac11 1–86 (WT and mutant) was incubated with 400 μM LC8. To test interaction of WT Pac11 1–86 with *S. cerevisiae* Dyn2, the methods listed above were implemented with the following differences. For the SEC interaction study, 400 μM WT Pac11 1–86 was incubated with 400 μM Dyn2 at 25°C for 2 hours and subsequently loaded onto a Superdex 75 10/300 GL (GE Healthcare). For the native PAGE analysis, Dyn2 and WT Pac11 1–86 were mixed in equimolar amounts (400 μM each).

Analytical ultracentrifugation

Preformed complexes were obtained from analytical gel filtration and subsequently used for sedimentation equilibrium analysis. Analysis was performed at 20°C using a Beckman-Coulter XLI Analytical Ultracentrifuge. Samples of individual proteins or protein complexes were dialyzed against 1× PBS and 1 mM TCEP (*Tris*(2-carboxyethyl) phosphine). Protein concentrations were analyzed between 0.1 and 0.6 $OD_{280/230}$ using three or more speeds. Samples were run between 10 and 25 μM Pac11 1–86 (WT and mutant constructs), each with 2 M excess of LC8. Equilibrium was assessed by radial scans at both 10 and 12 h during the each speed. Data was analyzed using Fast Fitter.

Yeast strain construction and methods

General yeast manipulation, media, and transformation were performed by standard methods (Amberg *et al.*, 2005). Strains are listed in Table S1. Gene-deletion and epitope-tag strains were constructed by PCR product-mediated transformation. Tags were placed at the 3′ end of the chromosomal ORF in haploid strains, and the expressed fusion proteins (Pac11–13Xmyc, Pac11-TAP, Dyn2–13Xmyc, Dyn2-GFP, Dyn2-mCitrine) were examined for function using cold-temperature spindle position assays, which assess dynein function by visualizing spindle orientation at low temperatures (12°C) using fluorescently labeled tubulin. All mutant strains containing fusion proteins behaved like the wild-type strain yJC5919 (containing GFP-Tub1), showing no spindle positioning defects in these assays. The light chain binding sites in Pac11 contain the following mutations: Pac11-VQ(51,52)DA, Pac11–DK(78,79)AA/IQ(81,82)DA, and Pac11-(51,52)DA/DK(78,79)AA/IQ(81,82)DA.

Bioinformatics

ClustalW2 at EMBL-EBI was used to create the alignments shown in Figure 3, B and C (Larkin *et al.*, 2007). PredictProtein was used for secondary structure analysis (Rost *et al.*, 2004).

Colony growth assay

Strains were grown to saturation (2–3 d) in liquid culture and serially diluted (fivefold dilution). Cultures were then transferred to YPD agar plates and allowed to grow for 1 or 2 d at 30°C and 23°C, respectively.

Fluorescence microscopy

Images of Dyn2 fluorescent chimeras were collected on an Olympus IX70 inverted fluorescence microscope with a ×100 N.A. 1.35 oil objective lens and a CoolSNAP HQ camera (Roper Scientific, Tucson, AZ) using QED software (Media Cybernetics, Silver Spring, MD). Living cells from asynchronous culture at early log phase were suspended in nonfluorescent medium and placed on an agarose pad as described (Waddle *et al.*, 1996). Microtubules were visualized with either CFP-Tub1 or GFP-Tub1 expressed from the TUB1 promoter integrated at the URA3 locus as described (Lee *et al.*, 2003) or at the LEU2 locus as described (Moore *et al.*, 2009), respectively. Dual fluorescence images were collected with an 86002bs v1 beam splitter cube (Chroma) to capture fluorescence from GFP and CFP sequentially.

Time-lapse Z-series images of spindle movement in HU-arrested cells were captured on an Olympus Bmax-60F microscope equipped with a 1.35NA 100× UPlanApo objective, spinning disk Confocal Scanner Unit (CSU10), Picarro Cyan laser (488 nm; Sunnyvale, CA), and a Stanford Photonics XR-Mega10 ICCD camera (Palo Alto, CA), using QED software (Media Cybernetics). A total of 16 confocal sections at 0.2-μm increments were captured every 15 s and collapsed into Z projections. Image analysis was performed using ImageJ (Rasband W.S., ImageJ, National Institutes of Health, Bethesda, MD, http://imagej.nih.gov/ij).

Fluorescence intensities of microtubule plus-ends were measured and corrected for background fluorescence with ImageJ as described (Moore *et al.*, 2008). Pixels immediately adjacent to the region of interest were used for background subtraction as described (Moore *et al.*, 2008).

Single–time point nuclear segregation assay

Saturated cultures were diluted 1:50 into 4 ml of fresh YPD and set at 12°C. After 20 h of shaking at 12°C, cells were quickly fixed in formaldehyde (final concentration 3.7% formaldehyde, 100 mM KPi) for 5 min. Cells were washed in Quencher solution (100 mM KPi, 0.1% Triton X-100, 10 mM ethanolamine) and then washed in 100 mM KPi. Cells were scored by counting the number of cells with normal and mispositioned spindle orientation as described (Moore *et al.*, 2009). Data were averaged from six independent experiments: ~300 cells were counted per experiment per strain.

Preanaphase spindle dynamics assay

Cells expressing GFP-Tub1 were grown to early log phase in synthetic media at 30°C. Cells were arrested in S phase by the addition of 200 mM HU. After 90 min of growth/shaking in HU, >90% of cells contained short bipolar spindles. Spindle movement in live cells was scored by collecting 38.75-min fluorescence movies, with images captured every 15 s. The position of the bud-proximal spindle pole was determined for each time point and compared with the position of the bud neck; distances were calculated by using ImageJ. Positive values represent a bud localized spindle pole, a zero value represents a bud neck localized spindle pole, and negative values represent a mother localized spindle pole.

Immunoprecipitations

Yeast cell cultures (20 ml) were inoculated and grown to an OD600 of ~0.7. The cultures were harvested, washed with water, and resuspended in 1 ml cold lysis buffer: 5 mM phosphate, pH 7.4, 140 mM NaCl, 0.1 mM DTT, and 0.2% Tween 20 (containing yeast protease inhibitor cocktail, 1 mM phenylmethylsulfonyl fluoride [PMSF], and 2 μg/μl aprotinin). Cells were lysed in 1.5-ml Eppendorf tubes with ~500 μl 0.5-mm glass beads (7 × 2 min) resulting in >95% lysis by phase contrast microscopy. Lysed cells were centrifuged at 4°C for 15 min at 13,200 rpm. Cell extracts were clarified in a Beckman TLA100.3 rotor at 50,000 rpm (103,320 × *g*) for 1 h at 4°C. Protein concentration of clarified lysates was determined using Bio-Rad Protein Assay (catalogue #500-0006). Next, 50 μl immunoglobulin G (IgG) Sepharose 6 Fast Flow (GE Healthcare catalogue #17-0969-01) was incubated with 3 mg of protein from each lysate for 1 h at 4C. Beads were washed three times with wash buffer 1: 5 mM phosphate, pH 7.4, 300 mM NaCl, and 0.4% Tween 20. Beads were then washed four times with wash buffer 2: 5 mM phosphate, pH 7.4, 140 mM NaCl, 0.2% Tween 20. All final wash buffer was removed, and the IgG Sepharose pellet was resuspended in 50 μl SDS loading buffer without βME (β-mercaptoethanol). Samples were boiled for 10 min and spun at 13,200 rpm for 5 min. Supernatant was separated from IgG Sepharose, and βME was added to supernatant sample prior to electrophoresis.

Immunoprecipitation samples were electrophoresed on a 10% acrylamide gel. Proteins were transferred to Immobilon-P^{SQ} (Millipore, Billerica, MA) PVDF membrane and blocked overnight with TBST (50 mM Tris-HCl, pH 8.0, 300 mM NaCl, and 0.05% Tween 20)

and 5% nonfat milk. Proteins were detected using rabbit α-TAP antibody (Open Biosystems catalogue #CAB1001) at a 1:1000 dilution and mouse α-myc antibody (Sigma M4439, clone 9E10) at a 1:2000 dilution (4 h incubation at room temperature) followed by secondary antibody incubation for 1 h at room temperature: goat α-mouse IgG–Peroxidase (Sigma A4416) and goat α-rabbit–peroxidase (Sigma A6154) both at a 1:10,000 dilution. Signals were detected using chemiluminescence.

ACKNOWLEDGMENTS

This work was supported by NIH Grant GM47337 (to J.A.C.) and by NIH Grant RR022316-01A1 (to J.C.W.). M.D.S.B. was supported by a postdoctoral fellowship from the Molecular Oncology program of the Siteman Cancer Center at Washington University and funded by NIH T-32-CA113275. A.E.S. was supported by the American Heart Association 0715196U.

REFERENCES

Amberg DC, Burke D, Strathern JN (2005). Methods in Yeast Genetics, Cold Spring Harbor, NY: Cold Spring Harbor Laboratory Press.

Barbar E, Kleinman B, Imhoff D, Li M, Hays TS, Hare M (2001). Dimerization and folding of LC8, a highly conserved light chain of cytoplasmic dynein. Biochemistry 40, 1596–1605.

Benashski SE, Harrison A, Patel-King RS, King SM (1997). Dimerization of the highly conserved light chain shared by dynein and myosin V. J Biol Chem 272, 20929–20935.

Benison G, Karplus PA, Barbar E (2007). Structure and dynamics of LC8 complexes with KXTQT-motif peptides: swallow and dynein IC compete for a common site. J Mol Biol 371, 457–468.

Breitkreutz A *et al*. (2010). A global protein kinase and phosphatase interaction network in yeast. Science 328, 1043–1046.

Campbell KS, Cooper S, Dessing M, Yates S, Buder A (1998). Interaction of p59fyn kinase with the dynein light chain, Tctex-1, and colocalization during cytokinesis. J Immunol 161, 1728–1737.

Dick T, Ray K, Salz HK, Chia W (1996a). Cytoplasmic dynein (ddlc1) mutations cause morphogenetic defects and apoptotic cell death in Drosophila melanogaster. Mol Cell Biol 16, 1966–1977.

Dick T, Surana U, Chia W (1996b). Molecular and genetic characterization of SLC1, a putative Saccharomyces cerevisiae homolog of the metazoan cytoplasmic dynein light chain 1. Mol Gen Genet 251, 38–43.

Espindola FS, Suter DM, Partata LB, Cao T, Wolenski JS, Cheney RE, King SM, Mooseker MS (2000). The light chain composition of chicken brain myosin-Va: calmodulin, myosin-II essential light chains, and 8-kDa dynein light chain/PIN. Cell Motil Cytoskeleton 47, 269–281.

Fan J, Zhang Q, Tochio H, Li M, Zhang M (2001). Structural basis of diverse sequence-dependent target recognition by the 8 kDa dynein light chain. J Mol Biol 306, 97–108.

Fan JS, Zhang Q, Li M, Tochio H, Yamazaki T, Shimizu M, Zhang M (1998). Protein inhibitor of neuronal nitric-oxide synthase, PIN, binds to a 17-amino acid residue fragment of the enzyme. J Biol Chem 273, 33472–33481.

Gee MA, Heuser JE, Vallee RB (1997). An extended microtubule-binding structure within the dynein motor domain. Nature 390, 636–639.

Gill SR, Cleveland DW, Schroer TA (1994). Characterization of DLC-A and DLC-B, two families of cytoplasmic dynein light chain subunits. Mol Biol Cell 5, 645–654.

Gross SP (2004). Hither and yon: a review of bi-directional microtubule-based transport. Phys Biol 1, R1–R11.

Habura A, Tikhonenko I, Chisholm RL, Koonce MP (1999). Interaction mapping of a dynein heavy chain. Identification of dimerization and intermediate-chain binding domains. J Biol Chem 274, 15447–15453.

Hall J, Hall A, Pursifull N, Barbar E (2008). Differences in dynamic structure of LC8 monomer, dimer, and dimer-peptide complexes. Biochemistry 47, 11940–11952.

Hall J, Karplus PA, Barbar E (2009). Multivalency in the assembly of intrinsically disordered Dynein IC. J Biol Chem 284, 33115–33121.

Hall J, Song Y, Karplus PA, Barbar E (2010). The crystal structure of dynein IC-light chain roadblock complex gives new insights into dynein assembly. J Biol Chem 285, 22566–22575.

Harrison A, King SM (2000). The molecular anatomy of dynein. Essays Biochem 35, 75–87.

Jaffrey SR, Snyder SH (1996). PIN: an associated protein inhibitor of neuronal nitric oxide synthase. Science 274, 774–777.

Kahana JA, Schlenstedt G, Evanchuk DM, Geiser JR, Hoyt MA, Silver PA (1998). The yeast dynactin complex is involved in partitioning the mitotic spindle between mother and daughter cells during anaphase B. Mol Biol Cell 9, 1741–1756.

Karki S, Holzbaur EL (1995). Affinity chromatography demonstrates a direct binding between cytoplasmic dynein and the dynactin complex. J Biol Chem 270, 28806–28811.

King SJ, Bonilla M, Rodgers ME, Schroer TA (2002). Subunit organization in cytoplasmic dynein subcomplexes. Protein Sci 11, 1239–1250.

King SJ, Brown CL, Maier KC, Quintyne NJ, Schroer TA (2003). Analysis of the dynein-dynactin interaction in vitro and in vivo. Mol Biol Cell 14, 5089–5097.

Kini AR, Collins CA (2001). Modulation of cytoplasmic dynein ATPase activity by the accessory subunits. Cell Motil Cytoskeleton 48, 52–60.

Koonce MP (1997). Identification of a microtubule-binding domain in a cytoplasmic dynein heavy chain. J Biol Chem 272, 19714–19718.

Lajoix AD, Gross R, Aknin C, Dietz S, Granier C, Laune D (2004). Cellulose membrane supported peptide arrays for deciphering protein-protein interaction sites: the case of PIN, a protein with multiple natural partners. Mol Divers 8, 281–290.

Larkin MA *et al*. (2007). Clustal W and Clustal X version 2.0. Bioinformatics 23, 2947–2948.

Lee WL, Kaiser MA, Cooper JA (2005). The offloading model for dynein function: differential function of motor subunits. J Cell Biol 168, 201–207.

Lee WL, Oberle JR, Cooper JA (2003). The role of the lissencephaly protein Pac1 during nuclear migration in budding yeast. J Cell Biol 160, 355–364.

Liang J, Jaffrey SR, Guo W, Snyder SH, Clardy J (1999). Structure of the PIN/LC8 dimer with a bound peptide. Nat Struct Biol 6, 735–740.

Lightcap CM, Sun S, Lear JD, Rodeck U, Polenova T, Williams JC (2008). Biochemical and structural characterization of the Pak1-LC8 interaction. J Biol Chem 283, 27314–27324.

Lo KW, Kan HM, Chan LN, Xu WG, Wang KP, Wu Z, Sheng M, Zhang M (2005). The 8-kDa dynein light chain binds to p53-binding protein 1 and mediates DNA damage-induced p53 nuclear accumulation. J Biol Chem 280, 8172–8179.

Lo KW, Naisbitt S, Fan JS, Sheng M, Zhang M (2001). The 8-kDa dynein light chain binds to its targets via a conserved (K/R)XTQT motif. J Biol Chem 276, 14059–14066.

Makokha M, Hare M, Li M, Hays T, Barbar E (2002). Interactions of cytoplasmic dynein light chains Tctex-1 and LC8 with the IC IC74. Biochemistry 41, 4302–4311.

McGrail M, Gepner J, Silvanovich A, Ludmann S, Serr M, Hays TS (1995). Regulation of cytoplasmic dynein function in vivo by the Drosophila Glued complex. J Cell Biol 131, 411–425.

Miller RK, Rose MD (1998). Kar9p is a novel cortical protein required for cytoplasmic microtubule orientation in yeast. J Cell Biol 140, 377–390.

Mok YK, Lo KW, Zhang M (2001). Structure of Tctex-1 and its interaction with cytoplasmic dynein IC. J Biol Chem 276, 14067–14074.

Moore JK, Li J, Cooper JA (2008). Dynactin function in mitotic spindle positioning. Traffic 9, 510–527.

Moore JK, Sept D, Cooper JA (2009). Neurodegeneration mutations in dynactin impair dynein-dependent nuclear migration. Proc Natl Acad Sci USA 106, 5147–5152.

Muhua L, Karpova TS, Cooper JA (1994). A yeast actin-related protein homologous to that in vertebrate dynactin complex is important for spindle orientation and nuclear migration. Cell 78, 669–679.

Navarro-Lerida I, Martinez Moreno M, Roncal F, Gavilanes F, Albar JP, Rodriguez-Crespo I (2004). Proteomic identification of brain proteins that interact with dynein light chain LC8. Proteomics 4, 339–346.

Neuwald AF, Aravind L, Spouge JL, Koonin EV (1999). AAA+: a class of chaperone-like ATPases associated with the assembly, operation, and disassembly of protein complexes. Genome Res 9, 27–43.

Nyarko A, Hare M, Hays TS, Barbar E (2004). The IC of cytoplasmic dynein is partially disordered and gains structure upon binding to light-chain LC8. Biochemistry 43, 15595–15603.

Nyarko A, Hare M, Makokha M, Barbar E (2003). Interactions of LC8 with N-terminal segments of the IC of cytoplasmic dynein. Scientific World Journal 3, 647–654.

Raux H, Flamand A, Blondel D (2000). Interaction of the rabies virus P protein with the LC8 dynein light chain. J Virol 74, 10212–10216.

Rodriguez-Crespo I, Yelamos B, Roncal F, Albar JP, Ortiz de Montellano PR, Gavilanes F (2001). Identification of novel cellular proteins that bind to

the LC8 dynein light chain using a pepscan technique. FEBS Lett 503, 135–141.
Rost B, Sander C (1994). Combining evolutionary information and neural networks to predict protein secondary structure. Proteins 19, 55–72.
Rost B, Yachdav G, Liu J (2004). The PredictProtein server. Nucleic Acids Res 32, W321–W326.
Samso M, Radermacher M, Frank J, Koonce MP (1998). Structural characterization of a dynein motor domain. J Mol Biol 276, 927–937.
Schroer TA (2004). Dynactin. Annu Rev Cell Dev Biol 20, 759–779.
Sheeman B, Carvalho P, Sagot I, Geiser J, Kho D, Hoyt MA, Pellman D (2003). Determinants of Scerevisiae dynein localization and activation: implications for the mechanism of spindle positioning. Curr Biol 13, 364–372.
Stelter P, Kunze R, Flemming D, Hopfner D, Diepholz M, Philippsen P, Bottcher B, Hurt E (2007). Molecular basis for the functional interaction of dynein light chain with the nuclear-pore complex. Nat Cell Biol 9, 788–796.
Susalka SJ, Nikulina K, Salata MW, Vaughan PS, King SM, Vaughan KT, Pfister KK (2002). The roadblock light chain binds a novel region of the cytoplasmic Dynein IC. J Biol Chem 277, 32939–32946.
Tai AW, Chuang JZ, Bode C, Wolfrum U, Sung CH (1999). Rhodopsin's carboxy-terminal cytoplasmic tail acts as a membrane receptor for cytoplasmic dynein by binding to the dynein light chain Tctex-1. Cell 97, 877–887.
Tynan SH, Gee MA, Vallee RB (2000). Distinct but overlapping sites within the cytoplasmic dynein heavy chain for dimerization and for IC and light IC binding. J Biol Chem 275, 32769–32774.
Vadlamudi RK, Bagheri-Yarmand R, Yang Z, Balasenthil S, Nguyen D, Sahin AA, den Hollander P, Kumar R (2004). Dynein light chain 1, a p21-activated kinase 1-interacting substrate, promotes cancerous phenotypes. Cancer Cell 5, 575–585.
Vallee RB, Williams JC, Varma D, Barnhart LE (2004). Dynein: an ancient motor protein involved in multiple modes of transport. J Neurobiol 58, 189–200.
Varma D, Dawn A, Ghosh-Roy A, Weil SJ, Ori-McKenney KM, Zhao Y, Keen J, Vallee RB, Williams JC (2010). Development and application of in vivo molecular traps reveals that dynein light chain occupancy differentially affects dynein-mediated processes. Proc Natl Acad Sci USA 107, 3493–3498.
Vaughan KT, Holzbaur EL, Vallee RB (1995). Subcellular targeting of the retrograde motor cytoplasmic dynein. Biochem Soc Trans 23, 50–54.
Vaughan KT, Vallee RB (1995). Cytoplasmic dynein binds dynactin through a direct interaction between the intermediate chains and p150Glued. J Cell Biol 131, 1507–1516.
Waddle JA, Karpova TS, Waterston RH, Cooper JA (1996). Movement of cortical actin patches in yeast. J Cell Biol 132, 861–870.
Williams JC, Roulhac PL, Roy AG, Vallee RB, Fitzgerald MC, Hendrickson WA (2007). Structural and thermodynamic characterization of a cytoplasmic dynein light chain-IC complex. Proc Natl Acad Sci USA 104, 10028–10033.
Williams JC, Xie H, Hendrickson WA (2005). Crystal structure of dynein light chain TcTex-1. J Biol Chem 280, 21981–21986.
Wu H, Maciejewski MW, Takebe S, King SM (2005). Solution structure of the Tctex1 dimer reveals a mechanism for dynein-cargo interactions. Structure 13, 213–223.
Yano H, Lee FS, Kong H, Chuang J, Arevalo J, Perez P, Sung C, Chao MV (2001). Association of Trk neurotrophin receptors with components of the cytoplasmic dynein motor. J Neurosci 21, RC125.